CIVIL ENGINEERING JOURNAL

Article no. 6

THE CIVIL ENGINEERING JOURNAL 1-2025

SIMULATION OF RC-T BEAM REINFORCED BY STEEL WIRE MESH AND POLYURETHANE CEMENT COMPOSITE (SWM-PUC)

Shiyu Chen, Kenxin Zhang, Dianye Cao, Yi Wang and Longsheng Bao

Shenyang Jianzhu University, School of Transportation and Geomatics Engineering, Shenyang, No.25 Hunnan Zhong Road, China; jt_zkx@sjzu.edu.cn

Received: 01.10.2024

Received in revised form: 05.12.2024

Accepted: 27.01.2025

ABSTRACT

In this paper, the flexural performance of seven steel wire mesh and polyurethane cement (SWM-PUC) composite-strengthened beams was investigated experimentally. The variation law of flexural performance of reinforced beams is clarified. Based on the experimental research, the deflection and stress analysis of SWM-PUC composite strengthened reinforced concrete beams was conducted using finite element analysis software ABAQUS. The Bending properties of reinforced beams with different steel wire mesh (SWM) reinforcement rates and different polyurethane cement (PUC) thickness parameters were researched.The finite element analysis shows that as the reinforcement ratio of the SWM increases, the yield and ultimate loads gradually increase and the deflection then gradually decreases. When the reinforcement ratio reaches a certain level, the increase in yield load decreases with the increase of the reinforcement ratio. As the thickness of the PUC increases, the yield limit and ultimate load gradually increase, and the deflection value decreases continuously. The optimum configuration of the SWM -PUC composite reinforcement layer was given through the finite element analysis.

KEYWORDS

Finite Element Analysis, Steel Wire Mesh, Polyurethane Cement, Reinforcement

INTRODUCTION

Nowadays, bridge deck pavement is prone to cracking, potholes and other problems under vehicle loads, temperature and environmental factors[1,2]. However, demolition and reconstruction of bridges is time-consuming and costly[3]. Therefore, to ensure that the existing bridge structure based on the bridge reinforcement can have considerable economic benefits at the same time can also produce good social benefits[4,5].

Stranded wire mesh (SWM) has good tensile strength, toughness and durability, often with polymer mortar as its bonding with concrete anchoring materials[6]. Polymer mortar has good film-forming properties and can adapt to the uneven surface of the reinforced concrete structure[7,8]. However, due to the relatively low strength of the polymer mortar, the composite reinforcement layer is prone to premature cracking, which negatively affects the durability of the SWM at the cracks[9-11]. And compared to polymer mortars, Polyurethane Cement (PUC) can make bridge reinforcement

more efficient and easier at a lower cost. In this way, the PUC material not only solves the problem of bonding to concrete but also provides additional reinforcement[12]. Shengran Zhang conducted an experimental study on PUC steel wire ropes in strengthening reinforced concrete structures. Findings show that PUC steel wire ropes can significantly improve the bearing capacity of reinforced concrete beams. The bearing capacity increases with the increase of the reinforcement ratio of the wire rope. The maximum increase in load-bearing capacity after reinforcement was 75.3%.

Although reinforcement methods such as steel wire mesh and polyurethane cement(SWM-PUC) composite reinforcement are costly, require professional skills and are highly affected by weather factors, they provide high strength and stiffness, good durability and corrosion resistance, convenient and fast construction, and are suitable for various structural forms[13-16]. The effects of various reinforcement techniques on reinforced elements can be obtained utilizing experimental methods[17,18]. However, to draw accurate conclusions, a large number of experiments would have to be carried out, which would be quite labor-intensive and costly. Therefore, it is necessary to simulate and analyze the reinforcement tests with the help of finite element software[19-21].

In this paper, an experimental study was conducted on seven reinforced concrete T-beams using SWM-PUC to improve the bending resistance of strengthened concrete beams. Based on the model, numerical analysis was conducted on SWM-PUC composite reinforced reinforced concrete beams using finite element analysis software ABAQUS. The effect of steel wire mesh (SWM) reinforcement rate and thickness of PUC on ultimate load was comparatively analyzed.

EXPERIMENTAL STUDY OF SWM AND PUC COMPOSITE REINFORCEMENT OF RC-T BEAMS FOR FLEXURAL RESISTANCE

Flexural Test Overview

A total of 7 Reinforced Concrete (RC) beams were designed in the experiment, of which 6 were composite reinforced beams and 1 was a beam that was not reinforced with SWM-PUC or Polymer mortar. The length of the beam is 3800 mm, the width of the upper flange is 360 mm and the height of the beam is 320 mm. The concrete strength grade is C30, the thickness of the protective layer is 25 mm, the longitudinal tensile reinforcement and the erection steel bars are HRB400 steel bars, and the distance of the loading point from the support is 1500 mm. The SWM used for reinforcement is a domestic galvanized strand type with a diameter of 2.4 mm. The main parameters of the test, besides the type of bonded anchorage material in the reinforcement layer, other reinforcement parameters such as SWM reinforcement ratio, PUC thickness, anchorage method and loading method were also considered. The design parameters of the specimens are presented in Table 1. The elevation details of the test beam are presented in Figure 1.

Tab.1 - Specimens design parameters

Beam	Bonded anchoring materials	Bonded anchoring materials thickness(mm)	Number of longitudinal steel wires	End anchoring method	Loading method
CB	-	-	-	-	-
B1	Polymer mortar	20	8	-	-
B2	Polymer mortar	20	8	End U-shaped anchorage	-
B3	PUC	20	5	-	-
B4	PUC	20	8	-	-
B5	PUC	30	5	-	-
B6	PUC	20	8	-	Preload

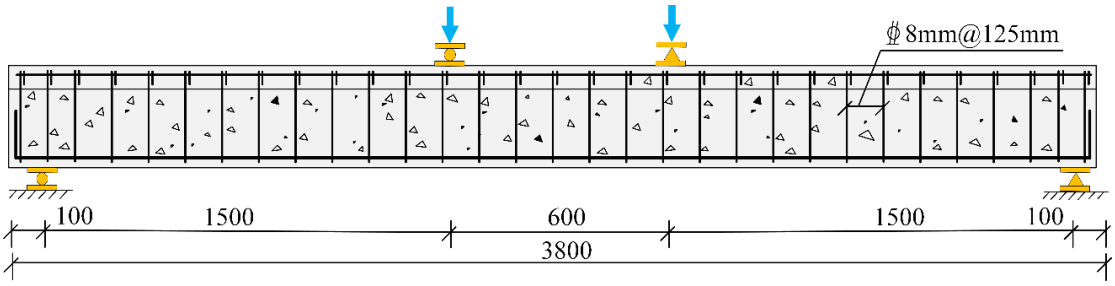

Fig. 2 – Elevation detail of test beam (unit: mm)

Test Measurement

The test used bow strain sensors to measure concrete strain and PUC strain, and resistance strain gauges to measure rebar strain and strand strain. Pre-load the test beam before testing formal loading, and check whether all test instruments and meters work normally. Before the beams cracked, they were loaded in 1 grade of 2kN. After cracks appeared in the concrete at the bottom of the beams, 1 loading level of 5kN was applied with a waiting time of 3 minutes to observe and record the test phenomena. All measurements are automatically recorded by the collection box. Once the bars were tied, an electrical resistance streak meter was installed at the center of each tensile bar. After the SWM has been stretched, one resistance strain gauge is arranged at the center of each longitudinal strand. The arrangement of the strain measurement points for reinforcement and strand in the elevation is shown in Figure 2. For the reinforced test beams, six strain measurement points were arranged along the length of the profile. The strain arrangement of the cross-section measurement points is shown in Figure 3.

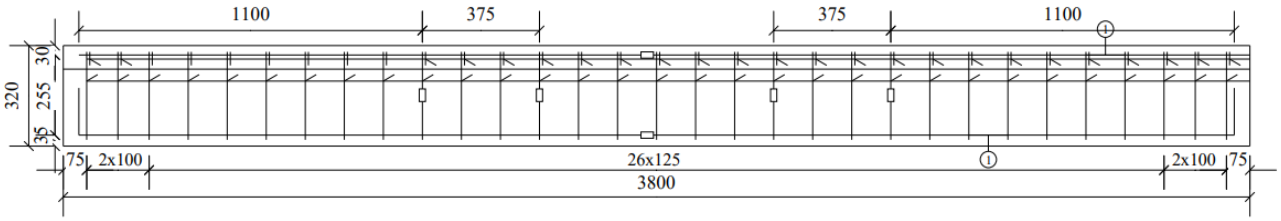

Fig. 2 – Reinforcing steel strand strain measurement point arrangement diagram

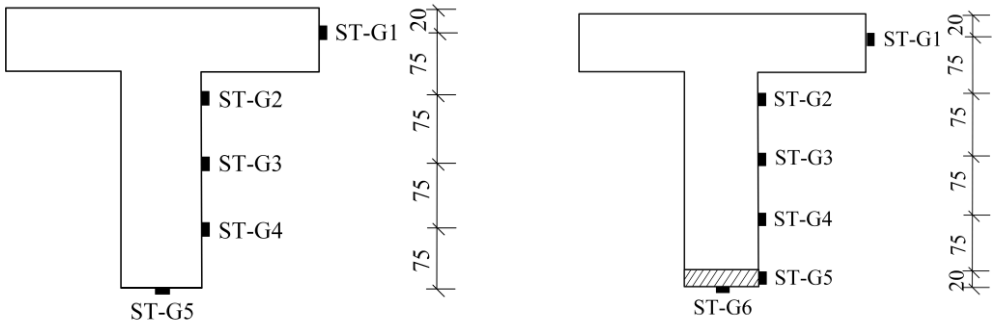

(a) – Unreinforced beam *(b) – Reinforced beam*

Fig. 3 – Concrete strain measurement point arrangement (unit: mm)

Test Results and Analysis

Load-Displacement Curve Analysis

The load-displacement curves of the specimens are presented in Figure 4. Reinforced beams are in an elastic working stage before cracking. Load is linearly related to displacement. The slopes

of the load-displacement curves were the same as those of the unreinforced comparison beams. After the cracks appear, the slope of the curve decreases, the stiffness of the section decreases and the deflection grows faster. The deflection increases more slowly in reinforced members than in unreinforced members. As the load increases, the reinforcement begins to yield. The slopes of the load-displacement curves of the unreinforced beams decrease sharply and the slopes of the load-displacement curves are almost horizontal. Due to the presence of the reinforcement layer, the load-displacement curve of the SWM and PUC composite reinforced members still has a large slope and the bearing capacity continues to grow. As the load continued to improve, the PUC material fractured with the SWM and the deflection of the members improved significantly.

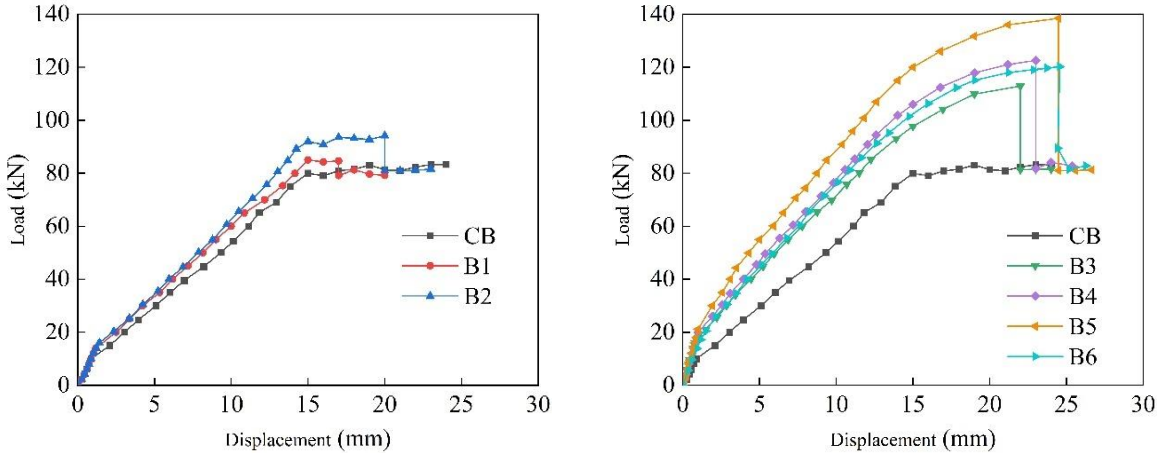

(a) – SWM-polymer mortar reinforcement specimens

(b) – SWM-PUC reinforcement specimens

Fig. 4 – Load-displacement curve

(1) Cracking load

The cracking load, yield load and ultimate load values for each test beam are presented in Table 2. The cracking load for the unreinforced beam CB is 10 kN. The cracking loads of beams B3, B4 and B5 were 18 kN, 20 kN and 22 kN, respectively, which were 80%, 100% and 120% higher than those of the unreinforced beams. The cracking load of the reinforced beams increases with the increase in the reinforcement ratio of the SWM. When the longitudinal strands were increased from 5 to 8, the cracking load of beam B4 increased by 2 kN compared to beam B3. Cracking loads increased with increasing thickness of PUC. When the thickness of the reinforcement layer was increased from 20 mm to 30 mm, the cracking load of beam B5 increased by 4 kN compared to beam B3. Therefore, SWM-PUC reinforcement can enhance the cracking load of beams. This is mainly because PUC and SWM together provide some reinforcement. The cracking load of beam B1 is 14 kN. The cracking load was reduced by 30% compared to beam B4 with the same SWM reinforcement ratio. The cracking load of beam B2 with end U-shaped anchorage was 16 kN. The cracking load was also reduced by 20% compared to beam B4 having the same SWM reinforcement ratio. It is shown that PUC materials are significantly better than polymer mortar materials for increasing the cracking loads of the test beams.

(2) Yield load

The output of the sensors is monitored in real-time by a data acquisition system to obtain the strain changes in the beam. On the stress-strain curve, find the point where the stress no longer increases linearly with strain, the yield point. Compared with unreinforced beams, the yield loads of beams B1 and B2 were improved by 16.6% and 25% respectively, and the yield loads of beams B3, B4, B5 and B6 were increased by 31.6%, 43%, 63.3% and 40% respectively. PUC has a greater increase in yield load than polymer mortar. It shows that PUC is more effective and significant in enhancing the yield load of reinforced beams. The yield load values of beams B3 and B4 were

increased by 31.6% and 43%, respectively, compared to the reinforced beams. It is shown that the magnitude of yield load enhancement increases with increasing reinforcement ratio of the SWM for the same reinforcement thickness. Compared to the reinforced beams, the yield load increase is 40% for the preloaded beam B6 and 43% for the unloaded beam B4. Both have almost the same lift for yield loads. It is shown that secondary stressed beams with initial damage also have better reinforcement.

(3) Ultimate load

From Table 2, it is shown that the ultimate load of the reinforced beams can be increased by up to 75% compared to the unreinforced beams. For beams B3, B4, B5 and B6 strengthened with SWM-PUC, the ultimate load increases were 41%, 53.3%, 75% and 50%, respectively. The ultimate load enhancement of B1 and B2 beams strengthened with SWM-polymer mortar increased by 6.3% and 17.5%, respectively. The former is more effective in increasing the ultimate load of the intensification beam. In addition, there is a 47 % difference in the lifting of the ultimate loads of beams B1 and B4. It is shown that PUC with strand reinforcement is more effective than polymer mortar with SWM reinforcement in enhancing the load-carrying capacity of the specimens. Beam B4 and Beam B6 have almost the same magnitude of lift for the ultimate load. It shows that the mode of loading has essentially no effect on the bearing capacity.

Tab.2 - Characteristic load test value

Beam	Cracking load/kN	Increase relative /%	Yield load/kN	Increase relative/%	Ultimate load/kN	Increase relative/%
CB	10	-	60	-	80	-
B1	14	40	70	16.6	85	6.3
B2	16	60	75	25	94	17.5
B3	18	80	79	31.6	112.8	41
B4	20	100	85.8	43	122.6	53.3
B5	22	120	98	63.3	140	75
B6	-	-	84	40	120	50

Load-Strain Curve Analysis

(1) Longitudinal reinforcement strain

The effect of reinforced concrete beams with SWM and two different materials was investigated by applying strain gauges to the reinforcement to measure the strain. It is shown in Figure 5 that the longitudinal reinforcement strain is linearly related to the load before cracking of the specimen. When the load reaches 40 kN, the strain of the unreinforced beam is 1585 με, and the strains of the SWM-polymer mortar beams B1 and B2 are 1288 με and 1127 με, respectively. The strains in beams B3, B4, B5 and B6 reinforced with SWM-PUC at this time were 853 με, 750 με, 697 με and 632 με, respectively. The SWM-PUC reinforcement specimens should be changed to a smaller size under the same load. The reason for this is that the SWM shares part of the load during loading, resulting in a smaller load increment in the reinforced beam for the same longitudinal strain. As the load increases, the reinforcement yields and the constraint of the SWM on the concrete become more pronounced. Continuing to increase the load, the strand mesh-polymer mortar reinforcement layer peeled away from the concrete, and the slope of its load-strain curve for the SWM was greatly reduced. However, the PUC remained well bonded to the concrete with a slow decrease in the slope of the load-reinforcement strain curve.

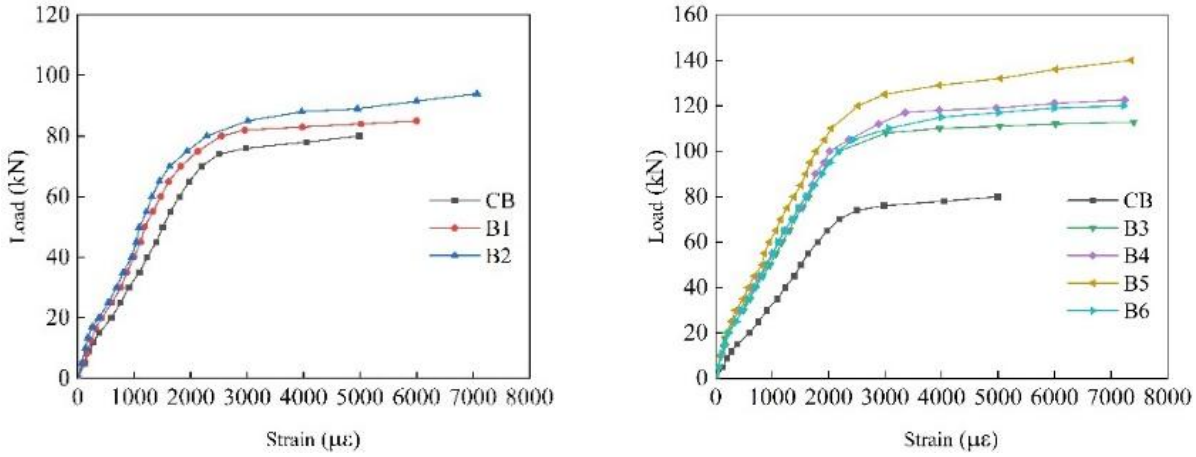

(a) – SWM-polymer mortar reinforcement specimens

(b) – SWM-PUC reinforcement specimens

Fig. 5 – Load-strain in reinforcement curves

(2) SWM strain

The load-strand strain curve is shown in Figure 6. From the figure, it is shown that the SWM is involved in the force throughout the loading process. Before the beam cracked, the load was linearly related to the strand strain. As the load increases, the crack develops and expands gradually, the neutralization axis moves upwards and the strain in the SWM increases gradually. When the reinforcement yields, the strain in the SWM increases rapidly. This is because the SWM exits the force and part of the load increment is carried by the SWM and the other part of the load increment is carried by the PUC. Until the composite reinforcement breaks. Among them, beams B1 and B2 were reinforced by SWM-polymer mortar, the SWM was not pulled off due to the stripping damage of the reinforcement layer from the concrete, and the strength of the SWM was not fully utilized.

(3) PUC strain

Based on the test data, the load-PUC strain curves for beams B3, B4, B5 and B6 were plotted as shown in Figure 7. As can be seen in Figure 7, the trend of load-PUC strains is the same for the test beams for the four different conditions. During the plastic working stage, the PUC strains of beams B3, B4, and B5 gradually decrease under the same loads. It shows that the stiffness of the test beam increases as the thickness of polyurethane increases. In this case, the load-PUC strain curves of beams B4 and B6 almost coincide, indicating that they have the same stiffness. It was further shown that the beams that were preloaded to produce cracks and then strengthened still had good stiffness. The same ultimate load capacity as the test beam that had not been pre-loaded. The ultimate damage loads of the test beams for the four different working conditions were 122.8 kN, 122 kN, 120 kN and 140 kN, at which time the corresponding PUC strains were 7000 με, 7140 με, 7071 με and 7336 με, respectively. PUC is known to have an ultimate tensile strain of 7000 με and a tensile strength of 35.6 MPa. The tensile stresses of beam B3, beam B4, beam B5 and beam B6 are 31.4 MPa, 32 MPa, 31.6 MPa and 32.2 MPa, respectively, which have reached the ultimate tensile strength of PUC. The damage to beam B3, beam B4, beam B5 and beam B6 were all composite reinforcement fractures. PUC has better bonding and tensile strength than polymer mortar and is more effective in increasing the load-carrying capacity of beams when reinforced with SWM.

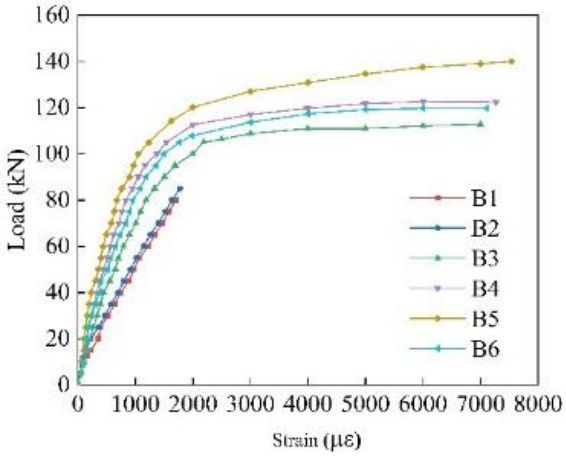

Fig.6 – Load-strand strain curve

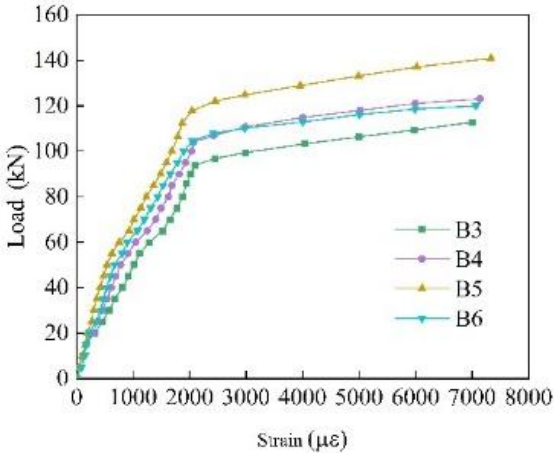

Fig.7 – Load-PUC strain curve

FINITE ELEMENT ANALYSIS OF SWM-PUC COMPOSITE REINFORCED RC-T BEAMS

Parameterisation of Materials

Concrete Unit and Parameter Setting

In this paper, a concrete plastic damage model is used, which can simulate the mechanical properties of concrete materials such as cracking and crushing. In this paper, the plasticity-based ontological relationship of concrete is used, as shown in Figure 8. The strain in the stress-strain curve of compressed concrete increases with increasing stress up to the maximum compressive strength, and eventually damage occurs when the ultimate strain is reached. The stress-strain curve of tensile concrete is linear until the maximum tensile strength is reached. After this, the concrete cracks and gradually decreases in strength. Poisson's ratio is 0.2. The modulus of elasticity is 30GPa.

$$\sigma_c = (1-d_c)E_c\varepsilon \tag{3.1}$$

$$d_c = \begin{cases} 1-\dfrac{p_c n}{n-1+x^n} & x \le 1 \\ 1-\dfrac{p_c}{a_c(x-1)^2+x} & x > 1 \end{cases}$$

$$p_c = \frac{f_c}{E_c\varepsilon_{c,r}}$$

$$n = \frac{E_c\varepsilon_{c,r}}{E_c\varepsilon_{c,r}-f_c}$$

$$x = \frac{\varepsilon}{\varepsilon_{c,r}}$$

$$\varepsilon_{c,r}=(700+172\sqrt{f_c})\times 10^{-6}$$

$$a_c = 0.157 f_c^{0.785} - 0.905$$

where d_c is the concrete uniaxial compression damage evolution parameters, E_c is the modulus of elasticity of concrete, a_c is the concrete uniaxial compression stress-strain curve descending section parameter section, f_c is the Concrete axial compressive strength, $\varepsilon_{c,r}$ is the Concrete axial compressive strength fc Corresponding peak compressive strain of concrete.

$$\sigma_t = (1-d_t)E_c\varepsilon \tag{3.2}$$

$$d_t = \begin{cases} 1-p_t(1.2-0.2x^5) & x \le 1 \\ 1-\dfrac{p_t}{a_t(x-1)^{1.7}+x} & x > 1 \end{cases}$$

$$p_t = \frac{f_t}{E_c\varepsilon_{t,r}}$$

$$x = \frac{\varepsilon}{\varepsilon_{t,r}}$$

$$\varepsilon_{t,r} = f_t^{0.54} \times 65 \times 10^{-6}$$

$$a_t = 0.312 f_t^2$$

where i_t is the concrete uniaxial tensile damage evolution parameters, a_t is the concrete uniaxial tensile stress-strain curve falling section parameter section, f_t is the concrete axial tensile strength, $\varepsilon_{t,r}$ is the concrete axial tensile strength ft corresponding concrete peak tensile strain.

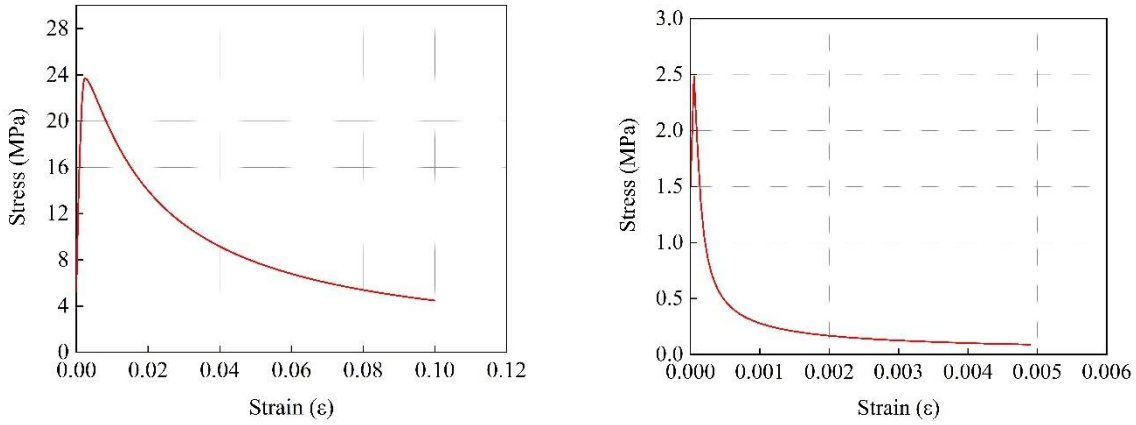

(a) – Axial compression *(b) – Axial tensile*

Fig. 8 – Constitutive relation of concrete

Rebar Unit and Strand Parameterisation

The common reinforcement required for this paper includes longitudinal bars, hoop bars, and erection bars. The intrinsic relationship adopted is a triple-fold model containing elastic, yield and strengthening phases. The strength of the bar continues to increase even after it reaches yield strength and enters the plastic phase. Es and Es* are the modulus of elasticity of the reinforcement in the elastic and strengthening phases, respectively. The simplified stress-strain curves of the steel bars are shown in Figure 9.

In this paper, measured strand stress-strain curves are used, as shown in Figure 10. SWM is hard and rigid in material, with almost no obvious plasticity section, its stress-strain curve pre-

approximate a straight line. When the applied load reaches the yield load of the SWM, the SWM enters the plastic phase and subsequently reaches the ultimate load. The SWM has a modulus of elasticity of 140GPa, an ultimate tensile strain of 0.0187 and a tensile strength of 1520 MPa.

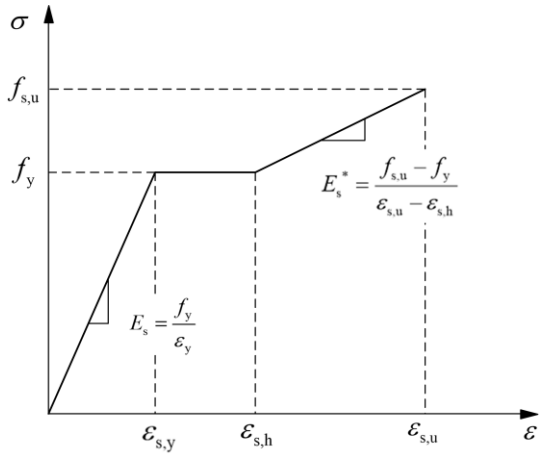

Fig. 9 – Reinforcement stress-strain simplified curve

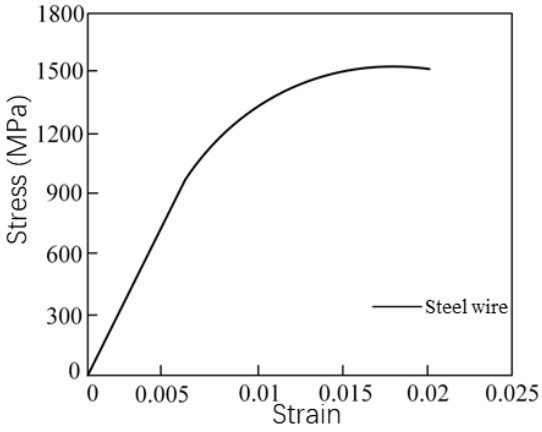

Fig. 10 – Steel-stranded wire axial tensile stress-strain curve

Properties and Parameters of PUC Material

In this study, the tensile intrinsic curve of PUC was obtained based on tests. According to the experimental results of PUC material, the modulus of elasticity of PUC material is taken as EPUC = 5500 MPA and Poisson's ratio is taken as v = 0.27. Figure 11 shows the measured axial tensile stress-strain curves for PUC materials. It is shown that in Figure 11, the ultimate tensile strain of PUC is 7000 με and the ultimate tensile stress of PUC is 35.6 MPa.

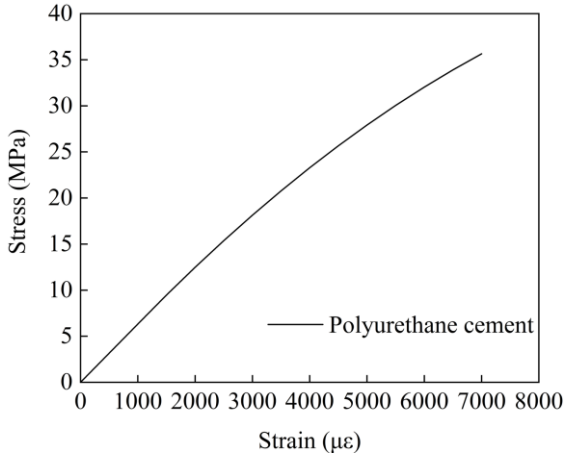

Fig. 11 – Measured axial tensile stress-strain curves of PUC materials

Finite Element Mechanism Analysis

Finite Element Modeling

The finite element units are selected as follows:

Solid units were selected for concrete, bearing pads and polyurethane cement; Selection of wire units for main reinforcement, hoop reinforcement and reinforcing strand mesh. See 3.1 for material parameter properties. In the model, the concrete and bearing pads are connected with a Tie, and the main reinforcement and rectangular hoop reinforcement in the concrete are embedded

in the Embedded region. The SWM is embedded in the polyurethane cement material using an Embedded region. Polyurethane cement material in contact with concrete select Tie. Constraints are added to the centerline of the pad by adding horizontal and vertical constraints at the supports to simulate simply supported beam boundary conditions.The mesh division size is 20mmx20mmx20mm and the model does not take into account the bond slip between the concrete and the reinforcement. A finite element model is established and the simulation results are compared and analyzed with the test results to verify the reliability of the simulation.

Deflection Analysis

Since the damage mode of the SWM-polymer mortar reinforced beams was peeling damage, the reinforcement and the SWM were not in full play and the results could not be analyzed accurately. Therefore, test beams B1 and B2 were not modeled. Unreinforced beams, beam B3, beam B4 and beam B5 were modeled and computationally analyzed to extract the deflections and ultimate deflections of the beams when the reinforcement yielded, respectively. The deflection clouds of beam CB, beam B3, beam B4 and beam B5 are shown in Figure 12.

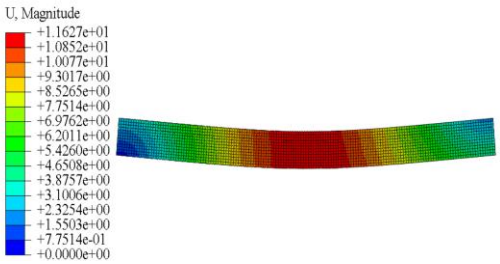

(a) – Deflection at yield of beam CB

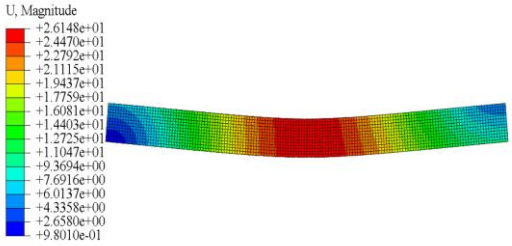

(b) – Deflection at limit state of beam CB

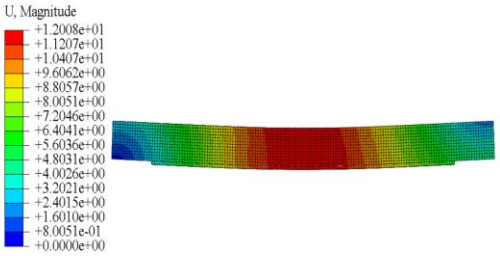

(c) – Deflection at yield of beam B3

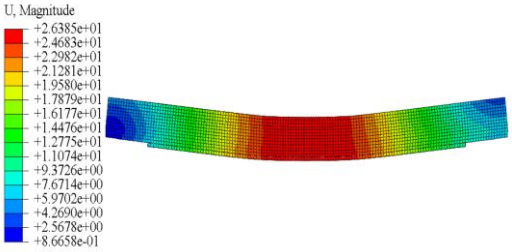

(d) – Deflection at limit state of beam B3

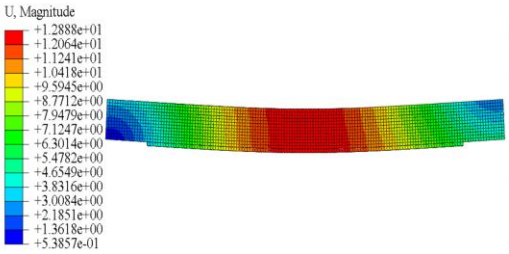

(e) – Deflection at yield of beam B4

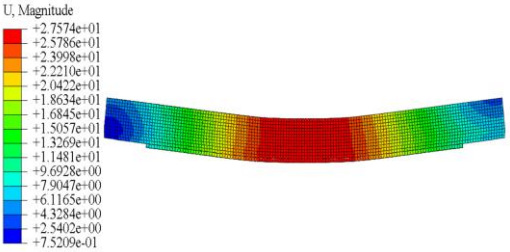

(f) – Deflection at limit state of beam B4

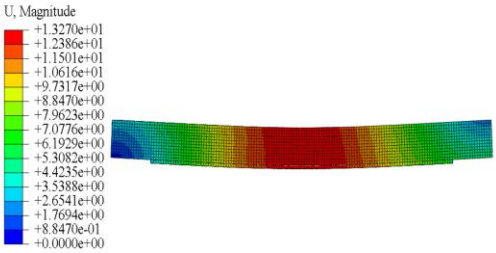

(g) – Deflection at yield of beam B5

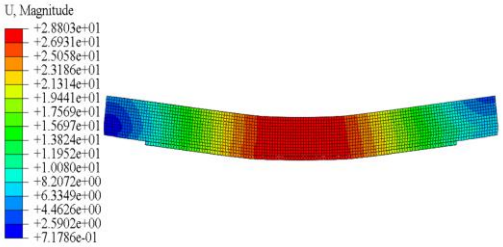

(h) – Deflection at limit state of beam B5

Fig.12 – Deflection clouds of beams CB, B3, B4 and B5

The unreinforced beam CB starts to yield its reinforcement when the load reaches 65 kN, at which point the deflection is 11.6 mm. Beam B3, which was strengthened using a combination of 5 longitudinal strands and 20mm thickness of PUC, entered the yield stage when the load reached 89.5 kN, at which point the deflection was 12 mm. The yield load was improved by 37.7% compared to the beam CB yield load. Beam B4, which was strengthened using a combination of 8 longitudinal strands and 20 mm thickness of PUC, had a load of 97 kN at the yield stage, at which point the deflection of the beam was 12.8 mm. The yield load is increased by 9% compared to beam B3. It shows that the yield load increases with the increase in reinforcement ratio for the same thickness of reinforcement. Beam B5, which was strengthened using a combination of 5 longitudinal strands and 30 mm thickness of PUC, had a load of 108 kN at the yield stage, at which point the deflection of the beam was 13.2 mm. The yield load is raised by 11.3% compared to beam B4. It shows that for the same thickness of reinforcement, the yield load increases with the increase in the thickness of reinforcement.

The ultimate load and ultimate deflection of beam CB are 78 kN and 26.1 mm respectively; The ultimate load and ultimate deflection of beam B3 are 117 kN and 26.4 mm respectively; The ultimate load and ultimate deflection of beam B4 are 130 kN and 27.6 mm respectively; The ultimate load and ultimate deflection of the B5 simulated beam were 144 kN and 28.8 mm respectively; Compared to beam CB, the ultimate loads of beams B3, B4, and B5 were enhanced by 50%, 67%, and 85%, respectively. Beam B4 with 8 longitudinal strands has an 11 % higher ultimate load compared to beam B3 with 5 longitudinal strands. It shows that the ultimate load increases gradually as the reinforcement ratio of the strand increases. Beam B5 with 30 mm thick PUC has a 10 % higher ultimate load compared to Beam B5 with 20 mm thick PUC. It can be seen that as the thickness of PUC increases, the ultimate load increases gradually.

Stress Analysis

(1) PUC stress

Through the post-processing module of ABAQUS finite element analysis software, the PUC stress clouds were extracted for each simulated beam reinforcement in the yield state and the limit state, as shown in Figure 13. The simulated beams for all three conditions went through yield and ultimate stages under load. Beam B3 strengthened with 5 longitudinal strands and 20 mm thick PUC had a stress of 11.9 MPa in the PUC at a load of 89.5 kN. At this point beam B3 enters the yield stage. The PUC stress is 31.4 MPa when the load reaches 117 kN. At this point the specimen reaches its limit state. Beam B4 strengthened with 8 longitudinal strands and 20 mm thick PUC had a stress of 12.3 MPa in the PUC at a load of 97 kN. At this point beam B3 enters the yield stage. The PUC stress is 32 MPa when the load reaches 130 kN. At this point the specimen reaches its limit state. Beam B5 strengthened with 5 longitudinal strands and 30 mm thickness of PUC had a stress of 13.4 MPa in the PUC at a load of 108 kN. At this point beam B3 enters the yield stage. At this point beam B3 enters the yield stage. The PUC stress is 32.4 MPa when the load reaches 144 kN. At this point the specimen reaches its limit state.

It is shown that the PUCs have all reached their ultimate stresses and fully utilized their strength. Moreover, as the reinforcement ratio of the SWM and the thickness of the PUC increase, the yield and ultimate loads gradually increase. The ultimate stresses of PUC in the simulated beams for all three conditions were much higher than the ultimate stresses of concrete. The PUC material proved to have good strength to meet the structural reinforcement needs.

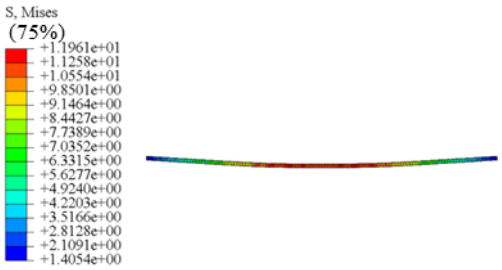

(a) – Stress in PUC at yield of beam B3

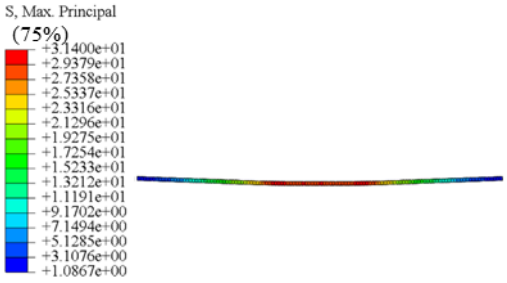

(b) – Limit state PUC stresses of the behavior of beam B3

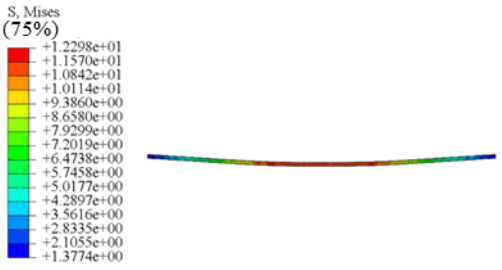

(c) – Stress in PUC at yield of beam B4

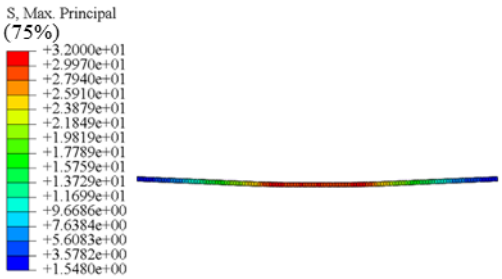

(d) – Limit state PUC stresses of the behavior of beam B4

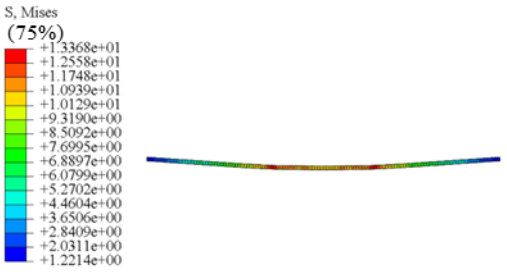

(e) – Stress in PUC at yield of beam B5

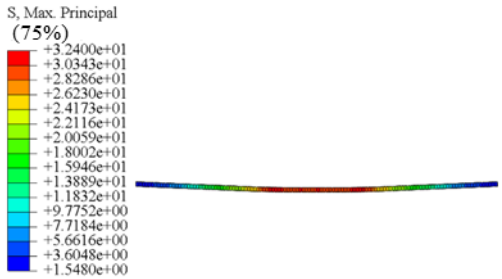

(f) – Limit state PUC stresses of the behavior of beam B5

Fig.13 – Stress clouds for PUC

(2) SWM stress

The strand stress clouds for beam B3, beam B4 and beam B5 are shown in Figure 14. Beam B3 begins to yield when the load reaches 89.5 kN, at which time the stress in the strand is 1140 MPa. Beam B4 strengthened with a composite of 8 longitudinal strands and 20 mm thickness PUC yielded its reinforcement at a load of 97 kN. The stress in the strand at this point is 1152 MPa. Beam B5 strengthened with a combination of 5 longitudinal strands and 30 mm thickness of PUC had a load of 108 kN at the yield stage. The stress in the strand at this point is 1160 MPa. This indicates that the strands in the reinforcement retained good strength when the specimen reached the yield state. In addition, the ultimate stresses of the strands in the reinforcement layers of beams B3, B4

and B5 all reached 1520 MPa, indicating that the form of damage of the beams was all bending damage in which the strands were pulled out.

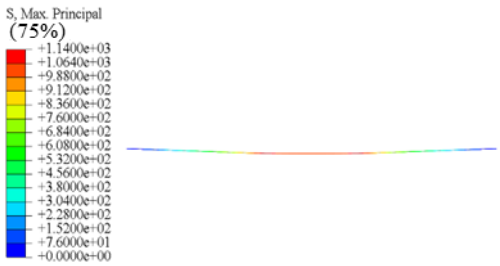

(a) – Strand stress at yield of beam B3

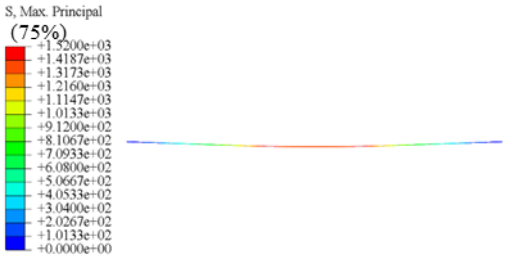

(b) – Strand stress of beam B3 at limit state

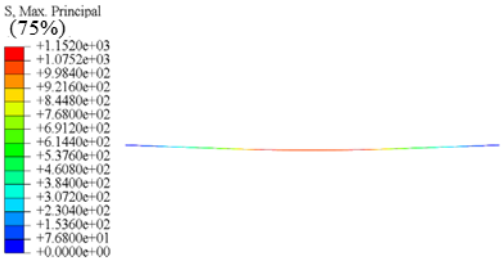

(c) – Strand stress at yield of beam B4

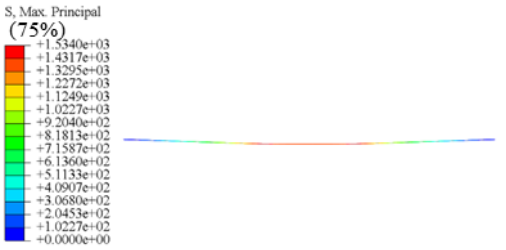

(d) – Strand stress of beam B4 at limit state

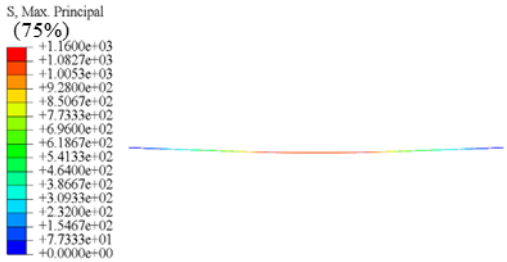

(e) – Strand stress at yield of beam B5

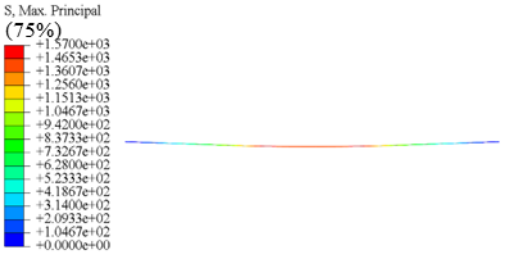

(f) – Strand stress of beam B5 at limit state

Fig.14 – Stress clouds of steel-stranded wires

(3) Reinforcement stress

The reinforcement stress clouds for beam CB, beam B3, beam B4 and beam B5 are shown in Figure 15. From Figure 15, it can be seen that the stresses in the rebars of the simulated specimens all exceeded 400 MPa, which reached the yield condition of the rebars. The stress is centered mainly at the underside of the reinforcement, indicating that the specimen has suffered bending damage. The ultimate stress of beam CB reinforcement is 440 MPa, beam B3 reinforcement is 500 MPa, beam B4 reinforcement is 521 MPa and beam B5 reinforcement is 555 MPa. Compared to beam CB, the tensile contribution of the reinforcement in beams B3, B4 and B5 was improved by 13.6%, 18% and 26%, respectively. It is shown that the composite reinforcement layer can appropriately increase the tensile contribution of the reinforcement. In addition, beam B4 with 8 longitudinal strands has 21 MPa more ultimate stress than the reinforcement of beam B3 with 5 longitudinal strands. It is shown that increasing the reinforcement ratio of the SWM can also increase the tensile contribution of the steel bars. Beam B5 with 30 mm thickness PUC had 55 MPa more ultimate stress in the reinforcement of beam B3 than that of beam B3 with 20 mm thick PUC. It is shown that an appropriate increase in the thickness of PUC can also improve the tensile contribution of the reinforcement.

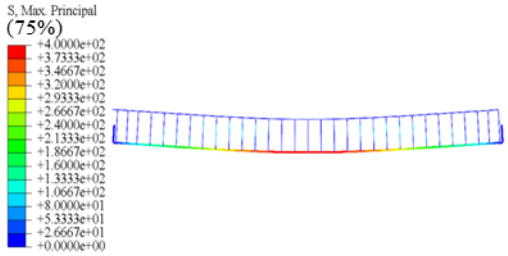

(a) – Reinforcement stress at yielding of beam CB

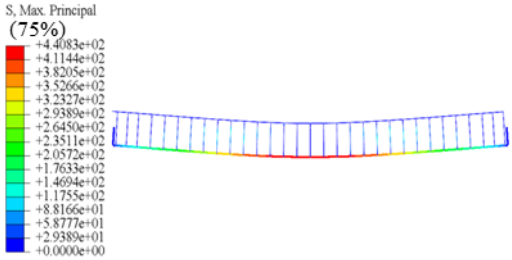

(b) – Steel reinforcement stresses of beam CB at limit state

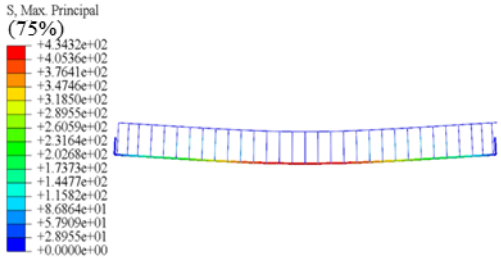

(c) – Reinforcement stress at yielding of beam B3

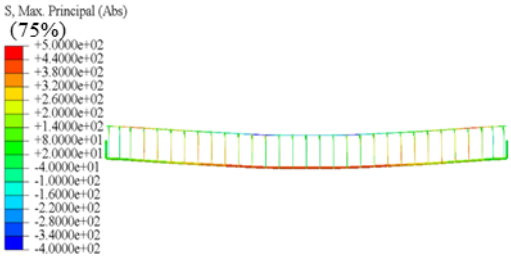

(d) – Steel reinforcement stresses of beam B3 at limit state

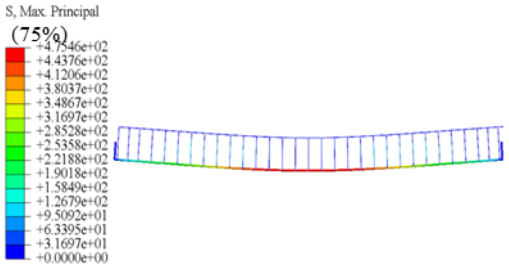

(e) – Reinforcement stress at yielding of beam B4

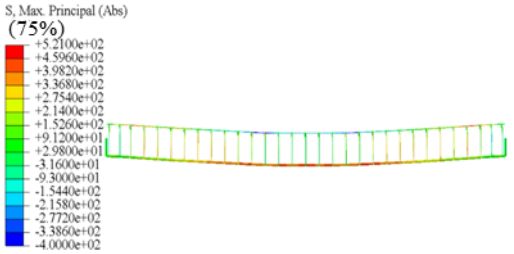

(f) – Steel reinforcement stresses of beam B4 at limit state

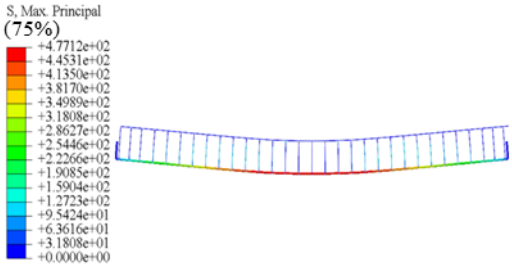

(g) – Reinforcement stress at yielding of beam B5

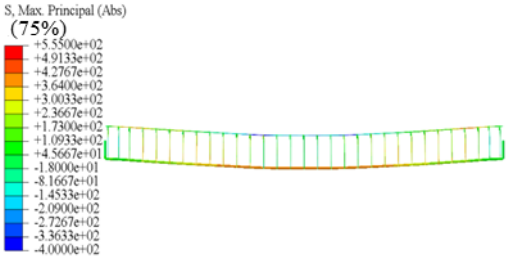

(h) – Steel reinforcement stresses of beam B5 at limit state

Fig.15 – Stress cloud of ordinary steel bar

Comparison of Load-Deflection Curves of Finite Element Model

After the finite element model analysis was completed, the finite element simulation results were compared with the test values as shown in Figure 16. From Figure 16, it is shown that the load-mid-span deflection curves of the finite element model have the same trend as the load-mid-span deflection curves of the test values, which are well-fitted.

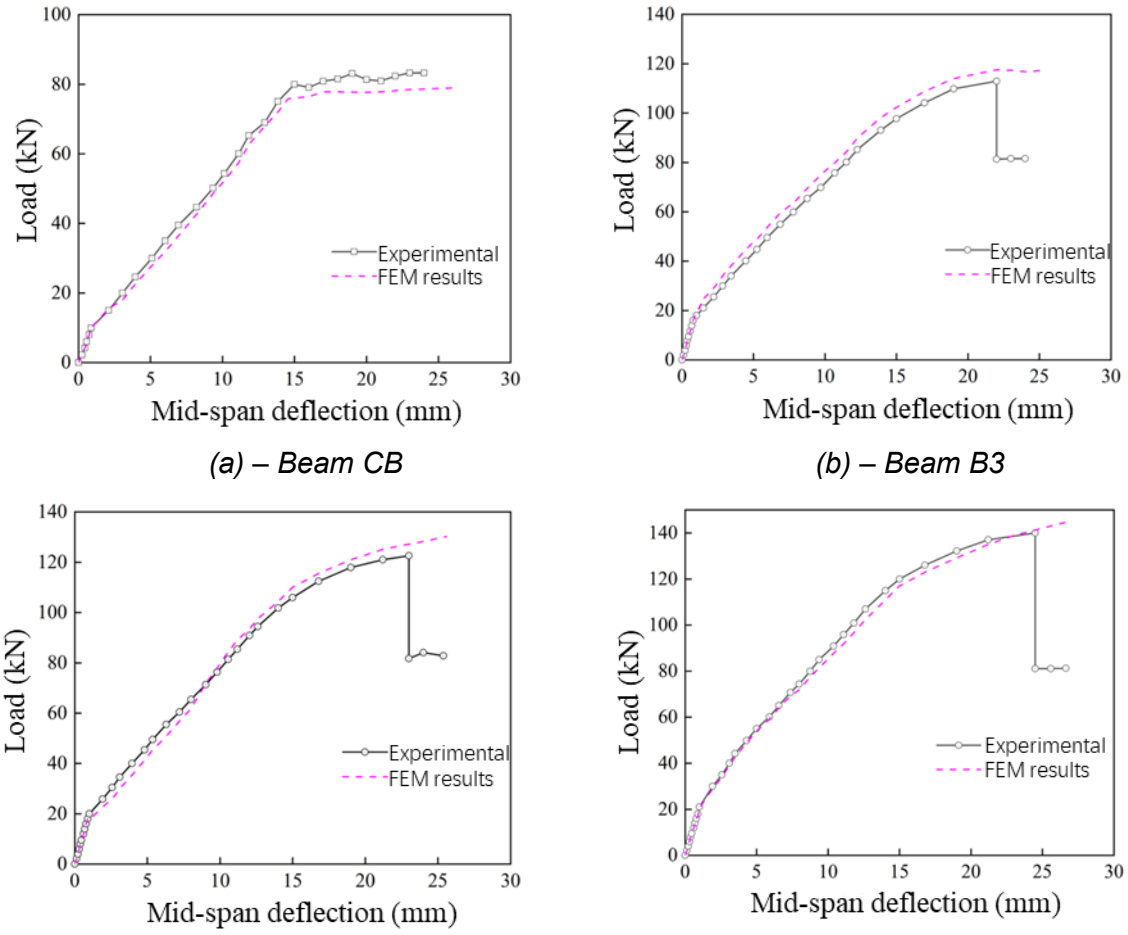

(a) – Beam CB

(b) – Beam B3

(c) – Beam B4

(d) – Beam B5

Fig. 16 – Load-deflection comparison curve of test value and finite element result

Analysis of Influencing Factors of Flexural Strengthened T-beams

Effect of Reinforcement Ratio of SWM on Reinforcement Performance

The SWM reinforcement ratio is defined as the ratio of the cross-sectional area of the longitudinal strands to the cross-sectional area of the upper unreinforced beams, which responds to the magnitude of the dosage of the SWM reinforcement ratio. The parameter settings for the simulated beams are shown in Table 3. All the parameters are the same except for the reinforcement ratio of the SWM. Eight longitudinal strands were used for each simulated beam, and the reinforcement ratio of the SWM was controlled by varying the diameter of the strands. The diameters of the longitudinal strands were 2.4 mm, 2.8 mm, 3.2 mm, 3.6 mm and 4 mm. The corresponding SWM reinforcement rates were 0.064%, 0.087%, 0.114%, 0.144% and 0.178%.

Tab.3 - Parameter setting

Beam	SWM reinforcement ratio	Longitudinal strand diameter/mm	Number of longitudinal strands/pc	Reinforcement layer thickness/mm	Tensile strength of SWM/MPa
WM-0.064	0.064%	2.4	8	20	1520
WM -0.087	0.087%	2.8	8	20	1520
WM -0.114	0.114%	3.2	8	20	1520
WM -0.144	0.144%	3.6	8	20	1520
WM -0178	0.178%	4	8	20	1520

The simulated beams with different SWM reinforcement rates were operated using finite element analysis software. The deflection values and load data were extracted respectively and the load-mid-span deflection curves were plotted. The load-deflection curves of the simulated beams with different SWM reinforcement ratios are shown in Figure 17. The trend of the load-deflection curves of the simulated beams with 5 different rates of SWM reinforcement was more or less the same, and all of them went through 3 phases, which were elastic, plastic, and destructive phases. The curve has a linear relationship between load and deflection in the first stage. As it becomes more loaded, the curve goes beyond the elastic phase and the curve slope decreases, at which point it enters the plastic phase. After exceeding the yield strength of the SWM, it enters the destruction phase. From Figure 17, it can be seen that the curve has a certain regularity. When the thickness of the reinforcement layer is constant, the rigid and bearing capacity of the simulated beam also increases with the increase of the reinforcement ratio of the SWM network.

The yield load values of the simulated beams with different SWM reinforcement rates are shown in Figure 18. The yield load of the simulated beam with a SWM reinforcement ratio of 0.064% is 92 kN; The yield load value of beam WM-0.087 is 104.6 kN, which is 13.7% higher than beam WM-0.064; The yield load value of beam WM-0.114 is 114.3 kN, which is 9.3% higher than the beam WM-0.087 yield load; The yield load value of beam WM-0.144 is 125 kN, which is 9.4% higher than the yield load of beam WM-0.114; The yield load value of beam WM-0.178 is 135 kN, which is 8% higher than the yield strength of beam WM-0.144. It is shown that the yield load increases gradually as the reinforcement ratio of the SWM increases. At a certain level of reinforcement, the increase in yield load decreases as the reinforcement rate increases.

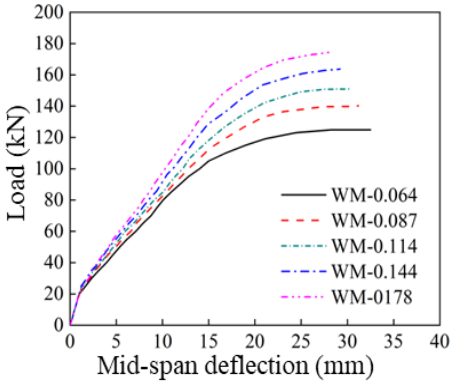

Fig.17 – Load-deflection curves of simulated beams of different SWM reinforcement ratios

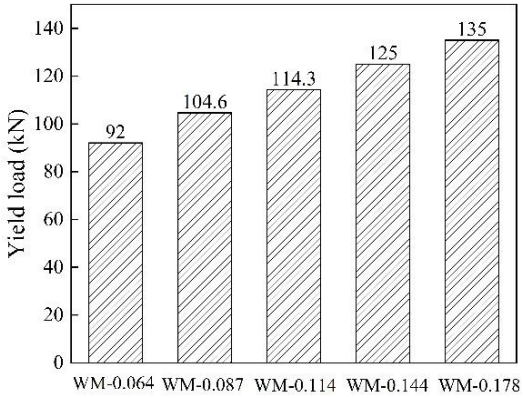

Fig.18 – Yield load values of simulated beams of different SWM reinforcement ratios

The ultimate load values of the simulated beams with different SWM reinforcement rates are shown in Figure 19. The ultimate loads of the SWM with 0.064%, 0.087%, 0.114%, 0.144% and 0.178% reinforcement were 122.6 kN, 139.5 kN, 152.5 kN, 166.7 kN and 180 kN. Compared to beam WM-0.064, with a 0.023% increase in the reinforcement ratio of the SWM, the ultimate load was increased by 13.8%; With a 0.05% increase in the reinforcement ratio of the SWM, the ultimate load was increased by 24.4%; With a 0.08% increase in the reinforcement ratio of the SWM, the ultimate load was increased by 36%; With a 0.114% increase in the reinforcement ratio of the SWM, the ultimate load was increased by 47%. It is shown that the ultimate load and the reinforcement ratio of the SWM are positively correlated.

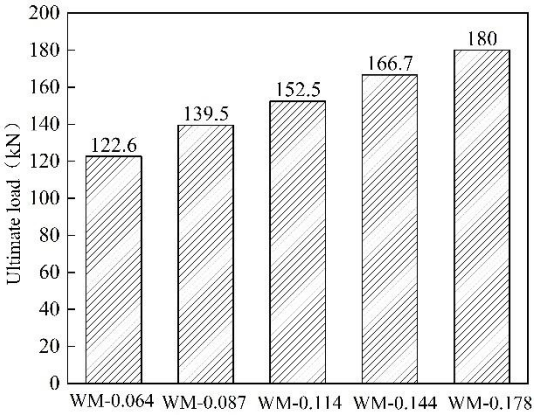

Fig.19 – Ultimate load values of simulated beams of different SWM reinforcement ratios

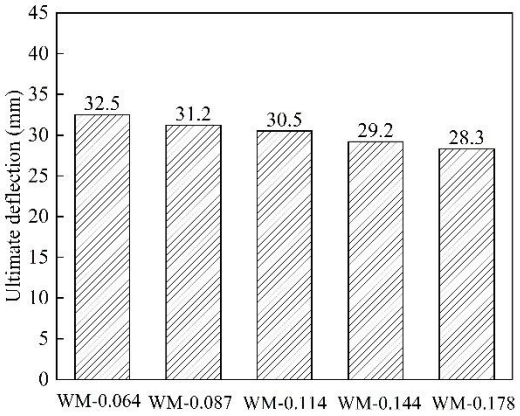

Fig.20 – Mid-span deflection values of the simulated beams while the strand is being pulled apart

After reinforcement with SWM-PUC composites. As the reinforcement ratio of the SWM increases, the deflection of the simulated beams decreases gradually under the same load. The mid-span deflection values of the simulated beams when the strand is pulled out are shown in Figure 20. The SWM reinforcement of 0.064%, 0.087%, 0.114%, 0.144% and 0.178% had deflections of 32.5 mm, 31.2 mm, 30.5 mm, 29.2 mm and 28.3 mm at the time of pull-off of the strand, respectively. Increasing the reinforcement ratio of the SWM decreases the flexural toughness of the beam. This is because increasing the reinforcement ratio will lead to an increase in the height of the compression zone of the cross-section and a decrease in the bending curvature, resulting in a decrease in the deformation capacity.

Effect of PUC Thickness on Reinforcement Performance

The PUC material was used as a composite reinforcement layer to increase the flexural load capacity of the specimen and firmly bonded to the concrete to avoid stripping damage. To verify the effect of PUC thickness on the flexural performance of reinforced beams in the positive section, simulated beams with different PUC thicknesses were established. The parameters are set as shown in Table 4. Parameters are the same except for PUC thickness. The PUC thicknesses were 20 mm, 25 mm, 30 mm, 35 mm and 40 mm.

Tab.4 - Parameter setting

Beam	PUC thickness/mm	Longitudinal strand diameter/mm	Number of longitudinal strands/pc	SWM reinforcement ratio	Tensile strength of SWM/MPa
PUC-20	20	2.4	5	0.064%	1520
PUC-25	25	2.4	5	0.064%	1520
PUC-30	30	2.4	5	0.064%	1520
PUC-35	35	2.4	5	0.064%	1520
PUC-40	40	2.4	5	0.064%	1520

The load-deflection curves of the simulated beams with different PUC thicknesses are shown in Figure 21. It is shown that the trend of the load-deflection curves of the simulated beams with different PUC thicknesses under all levels of loading is more or less the same, and all of them consist of elastic phase, plastic phase, and ultimate phase. The deflection in the span decreases as the thickness of PUC increases under the same load. In addition, the greater the thickness of PUC the greater the flexural capacity of the simulated beams. From Figure 21, it is shown that at a certain reinforcement rate of the SWM, the stiffness and load-carrying capacity of the simulated beams increased as the thickness of PUC increased.

The yield load values of the simulated beams with different PUC thicknesses are shown in Figure 22. The simulated beam reinforced with 20 mm thickness PUC enters the yielding stage when the load reaches 90.9 kN, at which point the deflection is 12.2 mm; The simulated beam with 25 mm thickness PUC enters the yielding stage when the load reaches 100.9 kN, at which point the deflection is 15.1 mm; The simulated beam with 30 mm thickness PUC enters the yielding stage when the load reaches 109.5 kN, at which point the deflection is 13 mm; The simulated beam with 35 mm thickness PUC enters the yielding stage when the load reaches 119.3 kN, at which point the deflection is 13.5 mm; The simulated beam with 40 mm thickness PUC enters the yielding stage when the load reaches 132 kN, at which point the deflection is 13.6 mm. The yield load is increased by 11% by adding 5 mm to the 20 mm thickness of PUC. The yield load is increased by 8.5% by adding 5 mm to the 25 mm thickness of PUC. The yield load is increased by 8.9% by adding 5 mm to the 30 mm thickness of PUC. The yield load is increased by 10.6 percent by adding 5 mm to the 35 mm thickness of PUC. It is shown that the yield load gradually increases as the thickness of PUC increases.

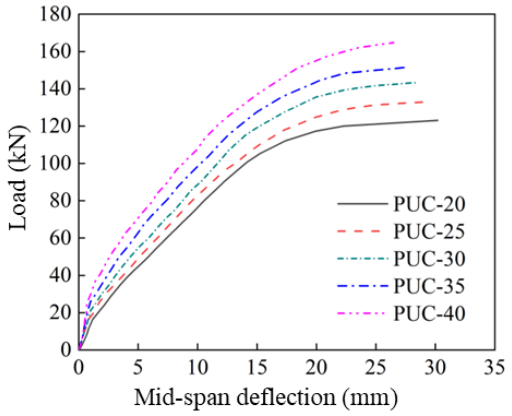

Fig.21 – Load-deflection curves of simulated beams of different PUC thicknesses

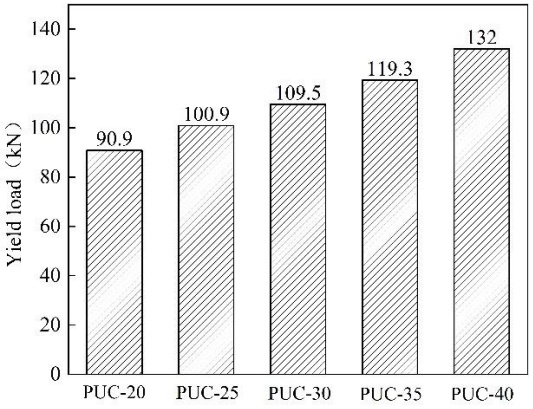

Fig.22 – Yield load values of simulated beams of different PUC thicknesses

The ultimate load values of the simulated beams with different PUC thicknesses are shown in Figure 23. The ultimate load of the PUC-20 simulated beam is 121.2 kN; The ultimate load of the PUC-25 simulated beam is 134.5 kN, which is 10.9% higher compared to the ultimate of the PUC-20 simulated beam; The ultimate load of the PUC-30 simulated beam is 146 kN, which is 8.5% higher compared to the ultimate load of the PUC-25 simulated beam; The ultimate load of the PUC-35 simulated beam is 159 kN, which is 8.9% higher compared to the ultimate load of the PUC-30 simulated beam; The ultimate load of the PUC-40 simulated beam is 176 kN, which is 10.7% higher compared to the ultimate load of the PUC-35 simulated beam. It can be seen that as the thickness of PUC increases, the ultimate load increases gradually. It is shown that PUC can be used not only as a bond anchoring material but also to reinforce the flexural properties of beams.

The mid-span deflection values of the simulated beams at PUC fracture are shown in Figure 24. The ultimate deflection of the simulated beam with PUC thickness of 20 mm is 30.2 mm; The ultimate deflection of the simulated beam with PUC thickness of 25 mm is 29.3 mm; The ultimate deflection of the simulated beam with PUC thickness of 30 mm is 28.6 mm; The ultimate deflection of the simulated beam with PUC thickness of 35 mm is 27.7 mm; The ultimate deflection of the simulated beam with PUC thickness of 40 mm is 26.5 mm. It is shown that as the thickness of PUC increases, the deflection of the simulated beams at failure gets smaller. The reason for this is that by increasing the thickness of PUC, the height of the compression zone in the cross-section of the reinforced beams under ultimate load increases. As the bending curvature becomes smaller, the deformation ability becomes worse, which leads to the reduction of toughness.

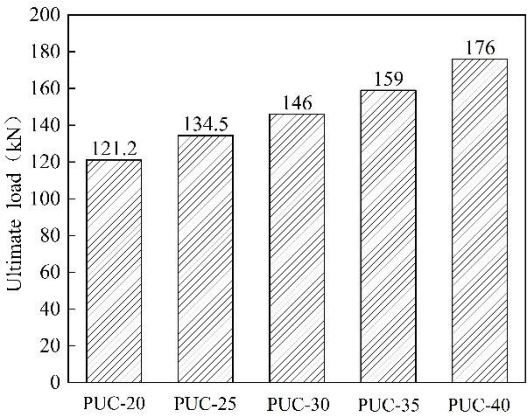

Fig.23 – Ultimate load values of simulated beams of different PUC thicknesses

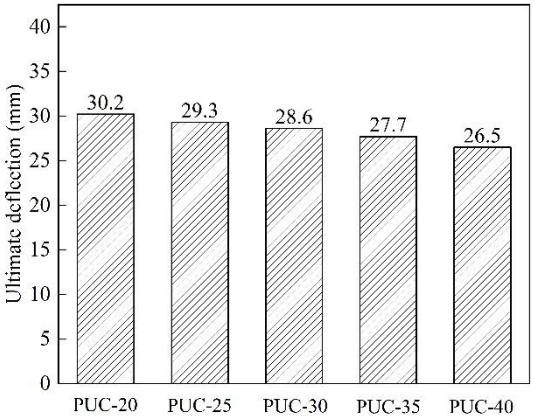

Fig.24 – Mid-span deflection values of the simulated beams at PUC fracture

From the results of the above analysis, it is concluded that the composite layer with PUC thickness of 40 mm and SWM reinforcement rate of 0.144% is the most effective reinforcement. The load-carrying capacity can be increased by up to 120 % compared to that of reinforced beams.

CONCLUSION

In this paper, the flexural performance of seven SWM-PUC composite strengthened beams was investigated experimentally. Based on the experimental study, the mechanical properties of strand mesh-polyurethane cement composite reinforced concrete beams were analyzed using finite element analysis software ABAQUS. The optimal strand mesh-polyurethane cement composite reinforcement layer configuration was explored. The following conclusions were drawn:

(1) A finite element model of a reinforced concrete T-beam with flexural reinforcement was developed using a simplified intrinsic relationship model of the material. The finite element results are in high agreement with the test results, indicating that the established SWM-PUC composite reinforcement beam model is reasonable.

(2) Computational analysis was carried out on reinforced concrete T-beam models with SWM reinforcement rates of 0.064%, 0.087%, 0.114%, 0.144%, and 0.178%. The results show a gradual increase in yield load as the reinforcement ratio of the SWM increases. However, at a certain level of reinforcement, the increase in yield load decreases as the reinforcement rate increases. With a 0.114% increase in the reinforcement rate of the SWM, the ultimate load was increased by 47% compared to the simulated beam with a 0.064% reinforcement rate of the SWM. It is shown that the ultimate load and the reinforcement ratio of the SWM are positively correlated.

(3) Computational analyses were carried out on reinforced concrete T-beam models with PUC thicknesses of 20 mm, 25 mm, 30 mm, 35 mm and 40 mm. It was concluded that for a certain reinforcement ratio of the SWM, the stiffness and load-carrying capacity of the beams increased as the thickness of PUC increased. Adding 10 mm to the 30 mm thickness of PUC increases the ultimate load by 20.5%. The optimum configuration of the SWM-PUC composite reinforcement layer was given by finite element analysis.

ACKNOWLEDGMENTS

The authors are grateful for the financial support of the Basic Research Projects of Liaoning Provincial Department of Education in 2024 (Project No. LJ212410153003), the Doctoral Start-up

Fund Projects of Liaoning Province (Project No. 2021-BS-168) and Shenyang Municipal Science and Technology Program Fund Project (23-407-3-19).

REFERENCES

[1] WANG, J., HE, X., et al. A real-time bridge crack detection method based on an improved inception-resnet-v2 structure. IEEE Access, 2021, 9, 93209–93223. DOI: 10.1109/ACCESS.2021.3093210.

[2] JIANG, H., FANG, Z., MA, Z. J., et al. Shear-friction behavior of groove interface in concrete bridge rehabilitation. *Journal of Bridge Engineering*, 2016, 21(11), 04016081. DOI: https://doi.org/10.1061/(ASCE)BE.1943-5592.0000953.

[3] ZHANG, S. S., YU, T., CHEN, G. M. Reinforced concrete beams strengthened in flexure with near surface mounted (NSM) CFRP strips: Current status and research needs. *Composites Part B: Engineering*, 2017, 131, 30-42. DOI: https://doi.org/10.1016/j.compositesb.2017.07.072.

[4] DE LORENZIS, L., TENG, J. G. Near-surface mounted FRP reinforcement: An emerging technique for strengthening structures. *Composites Part B: Engineering*, 2007, 38(2), 119-143. DOI: https://doi.org/10.1016/j.compositesb.2006.08.003.

[5] FANG, R., YANG, X. Cause and countermeasure of structure disease of bridge. In: *ICTIS 2013: Improving Multimodal Transportation Systems-Information, Safety, and Integration*. 2013, p. 470-475. DOI: https://doi.org/10.1061/9780784413036.064.

[6] LIU, Z. Q., GUO, Z. X., YE, Y. Flexural behaviour of RC beams strengthened with prestressed steel wire ropes polymer mortar composite. *Journal of Asian Architecture and Building Engineering*, 2022, 21(1), 48-65. DOI: https://doi.org/10.1080/13467581.2021.1928508.

[7] XING, G., WU, T., LIU, B. Experimental investigation of reinforced concrete T-beams strengthened with steel wire mesh embedded in polymer mortar overlay. *Advances in Structural Engineering*, 2010, 13(1), 69-79. DOI: http://dx.doi.org/10.1260/1369-4332.13.1.69.

[8] YUAN, F., CHEN, M., PAN, J. Flexural strengthening of reinforced concrete beams with high-strength steel wire and engineered cementitious composites. *Construction and Building Materials*, 2020, 254, 119284. DOI: https://doi.org/10.1016/j.conbuildmat.2020.119284.

[9] FISCHER, G., LI, V. C. Effect of fiber reinforcement on the response of structural members. *Engineering Fracture Mechanics*, 2007, 74(1-2), 258-272. DOI: https://doi.org/10.1016/j.engfracmech.2006.01.027.

[10] RANADE, R., LI, V. C., HEARD, W. F. Tensile rate effects in high strength-high ductility concrete. *Cement and Concrete Research*, 2015, 68, 94-104. cc DOI: https://doi.org/10.1016/j.cemconres.2014.11.005.

[11] WANG, X., YANG, G., QIAN, W. Tensile behavior of high-strength stainless steel wire rope (HSSSWR)-reinforced ECC. *International Journal of Concrete Structures and Materials*, 2021, 15(1), 1-15. DOI: https://doi.org/10.1186/s40069-021-00480-x.

[12] ZHENG, Y. Z., WANG, W. W., BRIGHAM, J. C. Flexural behaviour of reinforced concrete beams strengthened with a composite reinforcement layer: BFRP grid and ECC. *Construction and Building Materials*, 2016, 115, 424-437. DOI: https://doi.org/10.1016/j.conbuildmat.2016.04.038.

[13] ZHANG, K., QI, T., ZHU, Z., et al. Strengthening of a reinforced concrete bridge with a composite of prestressed steel wire ropes embedded in PUC. *Journal of Performance of Constructed Facilities*, 2021, 35(5), 04021063. DOI: https://doi.org/10.1061/(ASCE)CF.1943-5509.0001640.

[14] ZHANG, K., XUAN, J., SHEN, X., et al. Investigating the flexural properties of reinforced concrete T-beams strengthened with high-strength SWM-PUC. *Journal of Bridge Engineering*, 2024, 29(5), 04024023. DOI: https://doi.org/10.1061/JBENF2.BEENG-6524.

[15] LI, B., LIU, H., JIAN, J., et al. Static load test analysis of T-beam bridge shear strengthening by prestressed steel wire rope embedded in PUC (PSWR-PUC). *Sustainability*, 2023, 15(13), 10514. DOI: https://doi.org/10.3390/su151310514.

[16] ZHANG, K. Flexural simulation analysis of RC T-girders strengthed with PUC-prestressed steel wire ropes. *Stavební obzor - Civil Engineering Journal*, 2021, 30(4). DOI: https://doi.org/10.14311/CEJ.2021.04.0069.

[17] DHAKAL, R. P., MAEKAWA, K. Reinforcement stability and fracture of cover concrete in reinforced concrete members. *Journal of Structural Engineering*, 2002, 128(10), 1253–1262. DOI: https://doi.org/10.1061/(ASCE)0733-9445(2002)128:10(1253).

[18] SŁOWIK, M. The analysis of failure in concrete and reinforced concrete beams with different reinforcement ratio. *Archive of Applied Mechanics*, 2019, 89, 885–895. DOI: https://doi.org/10.1007/s00419-018-1476-5.

[19] NASER, M. Z., HAWILEH, R. A., ABDALLA, J. Modeling strategies of finite element simulation of reinforced concrete beams strengthened with FRP: A review. Jour*nal of Composites Science*, 2021, 5(1), 19. DOI: https://doi.org/10.3390/jcs5010019.

[20] FARON, A., ROMBACH, G. A. Simulation of crack growth in reinforced concrete beams using extended finite element method. *Engineering Failure Analysis*, 2020, 116, 104698. DOI: https://doi.org/10.1016/j.engfailanal.2020.104698.

[21] ALI, A. H., GOUDA, A., MOHAMED, H. M., et al. Nonlinear finite elements modeling and experiments of FRP-reinforced concrete piles under shear loads. In: *Structures*. Elsevier, 2020, 28, 106–119. DOI: https://doi.org/10.1016/j.istruc.2020.08.047.